



Structural and Energetic Consequences of Mutations in a Solvated Hydrophobic Cavity

D. H. Adamek*, L. Guerrero, M. Blaber and D. L. D. Caspar

*Institute of Molecular
Biophysics, Florida State
University, Tallahassee
FL 32306-4380, USA*

The structural and energetic consequences of modifications to the hydrophobic cavity of interleukin 1-beta (IL-1 β) are described. Previous reports demonstrated that the entirely hydrophobic cavity of IL-1 β contains positionally disordered water. To gain a better understanding of the nature of this cavity and the water therein, a number of mutant proteins were constructed by site-directed mutagenesis, designed to result in altered hydrophobicity of the cavity. These mutations involve the replacement of specific phenylalanine residues, which circumscribe the cavity, with tyrosine, tryptophan, leucine and isoleucine. Using differential scanning calorimetry to determine the relative stabilities of the wild-type and mutant proteins, we found all of the mutants to be destabilizing. X-ray crystallography was used to identify the structural consequences of the mutations. No clear correlation between the hydrophobicities of the specific side-chains introduced and the resulting stabilities was found.

© 2004 Elsevier Ltd. All rights reserved.

Keywords: protein packing; protein folding; protein hydration; aromatic hydrogen bond; beta trefoil

*Corresponding author

Background

The extent and nature of hydration of the interior regions of proteins continues to be a subject of great interest and considerable controversy. Internal protein hydration is of particular interest in cases where “packing defects” result in the presence of a cavity in the protein’s core.^{1–4} Considerable effort has been focused on understanding the energetic contributions of cavities in proteins and the implications for the hydrophobic effect. Several studies have focused on the structural and energetic consequences of creating cavities by replacing large aliphatic residues with smaller ones.^{5–10} Few of these cases result in the apparent hydration of the introduced cavity even though the cavities are generally lined with some polar atoms. The probability of finding a single water molecule in a small hydrophobic cavity has been estimated to be about 1 in 20,000.³ Clearly, for water to be stable within a protein cavity the environment therein must be energetically favorable relative to liquid water. Two factors that correlate closely to the ordered water content in interior and interfacial

protein cavities are the number of polar atoms lining the cavity and the cavity size, i.e. generally, larger more polar cavities are more hydrated.¹¹ Interleukin 1-beta (IL-1 β) contains an entirely hydrophobic cavity, defined by seven aliphatic residues and three phenylalanine residues, whose volume is large enough to accommodate about four water molecules. NMR studies revealed the presence of water within this cavity that had gone unrecognized in three previous X-ray crystal structures.⁴ A more recent crystallographic examination recognized the presence of approximately two positionally disordered water molecules.² Studies by Covalt *et al.* indicate a critical role of ordered buried water molecules to the folding and stability of the protein.¹² Though the energetics of solvating the cavity have been rationalized, a sufficient characterization of the internal environment remains unrealized. A common approach to probing the hydrophobic nature of a protein core is to introduce polar or charged residues into the region of interest.^{13–17} In general, such experiments result in significant destabilization, due primarily to the unfavorable desolvation energies associated with moving such residues from aqueous to apolar environments.^{18,19} Similarly, packing effects are often studied by examining the energetic and structural effects of replacing specific side-chains with smaller or larger ones.

Abbreviations used: DSC, differential scanning calorimetry; IL-1 β , interleukin 1-beta.

E-mail address of the corresponding author:
daniel.adamek@msfc.nasa.gov

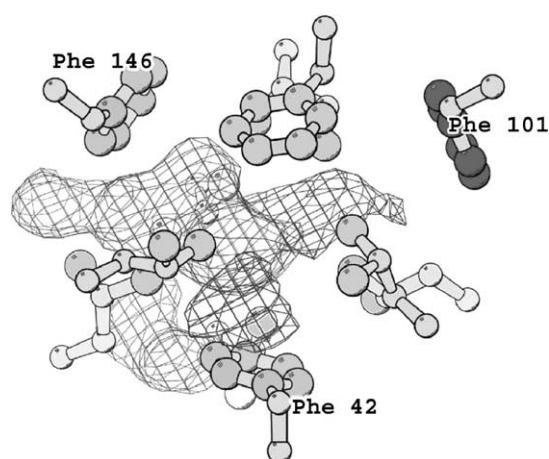


Figure 1. Ball and stick diagram of the cavity residues of wild-type IL-1 β . The wire contour represents positionally disordered water observed crystallographically. The triad of phenylalanine residues that circumscribe the cavity are shown in gray. Phenylalanine 101 (dark gray) is not solvent-accessible from the cavity. All other residues shown in light grey are the residues that form the cavity. Image adapted from Yu *et al.*²

Here, we report the energetic and structural consequences of introducing residues that modify the hydrophobic character of the cavity. Each of the three pseudo-symmetrically related phenylalanine residues that surround the cavity has been replaced with tyrosine, tryptophan, leucine and isoleucine by site-directed mutagenesis (Figure 1). X-ray crystal structures of the stable constructs are

examined. Differential scanning calorimetry (DSC) has been used to examine the relative stabilities of the wild-type and mutant proteins.

Results

Eleven mutant IL-1 β constructs are discussed. They are designated F42Y, F101Y, F146Y, F42W, F101W, F146W, WWW, F101I, F146I, F101L and F146L. The number represents the amino acid sequence position and the last letter represents the amino acid replacement. WWW is a triple tryptophan mutation where each of the phenylalanine residues at positions 42, 101 and 146 has been replaced. All of the constructs were confirmed by DNA sequence analysis.

DSC studies

Wild-type IL-1 β

Calorimetric examination of protein folding is optimally done under conditions where equilibrium between thermodynamic states of the system is attainable throughout the temperature range of the experiment. Under neutral conditions IL-1 β aggregates and precipitates when unfolded by temperature. However, at lower pH (\sim 2–3) IL-1 β demonstrates thermal unfolding that is highly reversible and closely approximates a two-state transition.²⁰ The drawback of lowering the pH to attain two-state thermal unfolding of IL-1 β is that it substantially destabilizes the protein.

Previous reports established that low concentrations of guanidine hydrochloride (GuHCl)

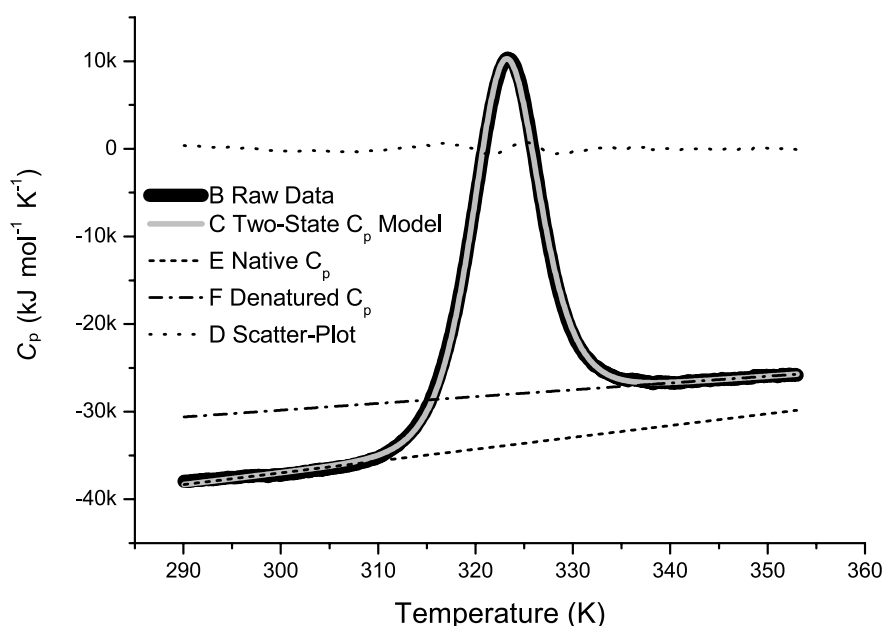


Figure 2. Differential scanning calorimetry data of wild-type IL-1 β . Profile (bold black) represents an average of three sample scans of protein. The overlaid gray line is a representative two-state model. The scatter plot reflecting the difference between the model and the data is the dotted line near the 0 C_p position. The lower broken line represents a linear fit to the native state heat capacity baseline. The dash-dot line represents a linear fit to the denatured state heat capacity baseline.

Table 1. Thermodynamic parameters obtained from DSC analyses

	Wild-type	F42Y	F101Y	F146Y	F42W	F101W	F146W	WWW
T_m (K)	322.8 \pm 0.1	305.6 \pm 0.9	314.9 \pm 0.1	315.3 \pm 0.1	320.0 \pm 0.1	320.3 \pm 0.1	322.1 \pm 0.1	317.3 \pm 0.2
ΔH (kJ/mol)	376 \pm 1	207 \pm 60	279 \pm 1	272 \pm 1	343 \pm 6	330 \pm 6	367 \pm 1	274 \pm 3
$\Delta H_{vH}/H_{cal}$	0.97	0.69	1.08	1.12	1.07	0.97	0.94	1.13
ΔC_p^{Tm} (kJ/mol K)	5.8 \pm 0.3	4.7 \pm 1.8	4.0 \pm 0.2	3.8 \pm 0.7	6.9 \pm 0.7	5.6 \pm 0.1	5.1 \pm 0.1	7.1 \pm 1.0
ΔG_{298}^{fold} (kJ/mol)	22.7 \pm 0.3	3.96 \pm 0.7	12.5 \pm 0.2	13.7 \pm 0.5	17.8 \pm 0.3	17.1 \pm 0.6	21.4 \pm 0.2	11.7 \pm 0.8
$\Delta\Delta G^{298}$ (kJ/mol)		-18.7	-10.2	-9.0	-4.9	-5.6	-1.3	-11.0
$\Delta\Delta G^{WT}$ (kJ/mol)		-18.5 \pm 0.7	-7.3 \pm 0.1	-6.8 \pm 0.1	-3.0 \pm 0.1	-2.6 \pm 0.1	-0.8 \pm 0.1	-5.10 \pm 0.2
SD (J/mol K)	278	1100	603	204	216	306	250	193

T_m is the transition midpoint or melting temperature. ΔH is the calorimetric enthalpy. $\Delta H_{vH}/H_{cal}$ is ratio of the van't Hoff to calorimetric enthalpies. $\Delta\Delta G^{25^\circ C}$ is the difference in the free energy of unfolding extrapolated to 25 °C between wild-type Il-1 β and the mutants. $\Delta\Delta G^{WT}$ is the free energy of unfolding of the mutants at the melting temperature of the wild-type protein.

can reduce or eliminate thermally induced aggregation.^{21,22} We found similar results with Il-1 β . The energetic cost, however, is much less than that suffered by lowering the pH. This is desirable, as our goals are to examine potentially destabilizing mutations.

The thermal unfolding of wild-type Il-1 β in 0.7 M GuHCl at a scan rate of 15 deg. C per hour is highly reversible, as indicated by about 90% recovery of folded sample after one thermal cycle, i.e. the calorimetric enthalpy of the second scan is 90% of that of the first scan. The calorimetric criterion for a two-state transition is met where the ratio of the van't Hoff enthalpy to calorimetric enthalpy ($\Delta H_{vH}/H_{cal}$) approximates unity (Figure 2). Thermodynamic parameters for all constructs are shown in Table 1.

Phe to Tyr mutants

Each of the threefold-related phenylalanine residues was individually replaced with tyrosine (Figure 3). The replacement at position 42 severely decreased the stability of the protein. In the absence of GuHCl this construct has very low solution

stability. Furthermore, the protein demonstrated severe freeze denaturation, where most of the protein was lost to precipitation upon thawing. However, in the presence of a low concentration of GuHCl the construct remains soluble indefinitely. The instability of this construct made study by DSC difficult. The unfolding transition is considerably broader than that of wild-type Il-1 β and the native state baseline is rather ill defined making analyses difficult. This is reflected in the large errors associated with thermodynamic parameters reported in Table 1. The $\Delta H_{vH}/H_{cal}$ of 0.69 may reflect some non-two-state behavior. The mutation results in a decrease in melting temperature of about 17 deg. C corresponding to a $\Delta\Delta G$ of approximately -18.5 kJ/mol.

Position 101 was able to accommodate the mutation to tyrosine with milder destabilization than that suffered by the F42Y mutant. The $\Delta H_{vH}/H_{cal}$ of 1.08 indicates that the unfolding approximates a two-state transition. The mutation results in a decrease in melting temperature of approximately 8 deg. C corresponding to a $\Delta\Delta G$ of 7.3 kcal/mol.

Replacing phenylalanine 146 with tyrosine yielded very similar results to the position 101

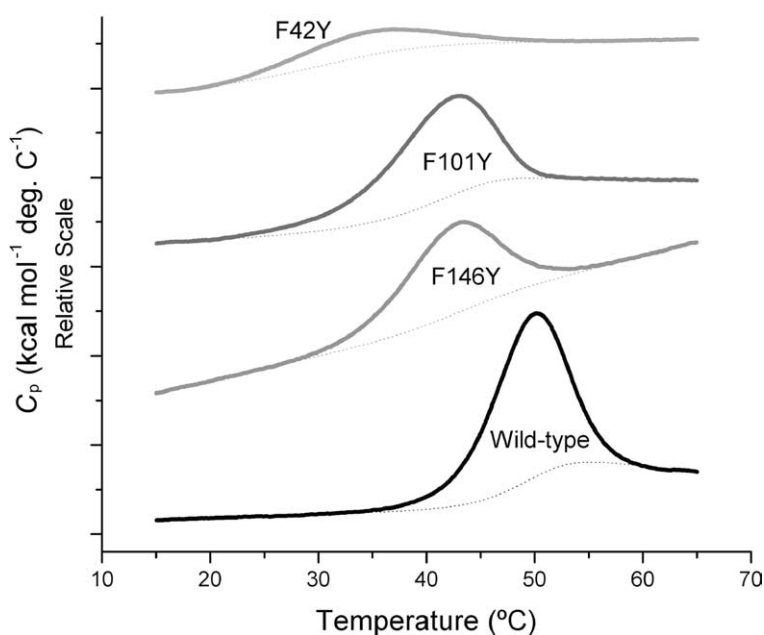


Figure 3. Heat capacity curves for tyrosine mutants. Each curve represents the average of three different sample scans. The dotted line below each curve is for visual reference. The area between the data profile and the reference line approximates the relative enthalpy of the unfolding transition.

mutation. DSC analysis of this mutant revealed some slightly anomalous behavior. The heat capacity continues to increase after the apparent unfolding transition. This may reflect the introduction of some appreciable non-two-state equilibrium behavior due to this mutation. Another possibility is that the kinetics may be sufficiently altered, such that the experimental parameters, namely the scan rate, optimized for the wild-type protein are not optimal for this particular mutant. Heidary *et al.* demonstrated that mutations to tryptophan at all three sites under investigation here significantly alter the folding kinetics.²³ While a more rigorous study of the scan rate dependence and the folding kinetics would elucidate better the nature of this behavior, for the purposes of this comparative study we have evaluated the fidelity of the data by their fit to the two-state model. This treatment of the data gives reasonable parameters, with only slightly greater error than that observed in the F101Y analysis and the unfolding still appears to approximate a two-state transition where $\Delta H_{vH}/H_{cal}$ of 1.12. The mutation results in a decrease in melting temperature of approximately 7.5 deg. C, corresponding to a $\Delta\Delta G$ -6.8 kcal/mol.

Phe to Trp mutants

Positions 42, 101 and 146 were replaced individually and in combination to produce three single-point tryptophan mutants and a triple tryptophan mutant (Figure 4). All of these mutations destabilized the protein, but to a lesser degree than the comparable tyrosine mutations. The melting temperatures of F42W, F101W, F146W and WWW were found to be 2.8, 2.5, 0.7 and 5.5 deg. C lower than that of the wild-type protein with relative free energy differences of -3.0 , -2.6 , -0.8 and -5.1 kJ/mol, respectively, where the negative value indicates a decrease in relative stability.

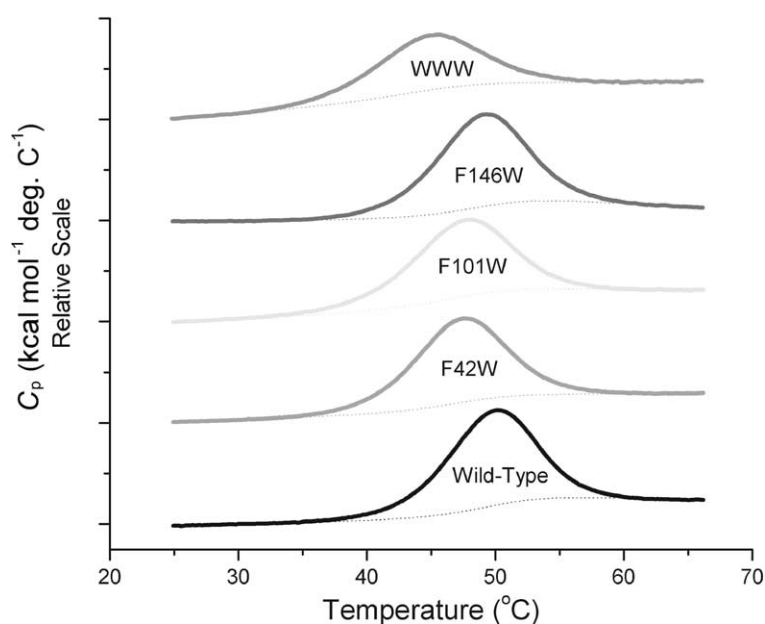


Figure 4. Heat capacity curves for tryptophan mutants. Each curve represents the average of three different sample scans. The dotted line below each curve is for visual reference. The area between the data profile and the reference line approximates the relative enthalpy of the unfolding transition.

Aliphatic replacement mutations

The phenylalanine residues at positions 42 and 146 were each replaced individually with leucine and isoleucine. None of the four resulting mutants was solution-stable. That is, precipitation could be observed within hours after the final purification step. The addition of 0.7 M GuHCl remedied this. However, the proteins demonstrated severe instability, as indicated by DSC and circular dichroism analysis (data not shown). These constructs were therefore impossible to quantitatively characterize. F146L was the only one of these constructs for which we observed an apparent cooperative transition. Even in this case the unfolding was irreversible and, due to the apparent decay of the protein over time, the results were irreproducible. Due to the lack of quantitative information that could be extracted from these samples under the described conditions no further studies of these constructs were pursued.

X-ray crystallography

Crystals of F101Y, F146Y, F42W, F101W, F146W, F146W and F101W-F146W-F146W grew under previously reported conditions for the wild-type protein to the same crystal morphology. X-ray data for all revealed the crystal lattice to be isomorphous to the wild-type IL-1 β . Due to decreased stability and solubility all attempts under a variety of conditions to crystallize F42Y, and all of the aliphatic mutants, resulted in amorphous precipitation of the protein. X-ray data and model statistics are reported in Table 2.

No gross structural changes were observed in any of the crystallized mutants. In each case the introduced polar atoms found hydrogen-bonding partners, without a significant change in the gross or local protein structure.

Table 2. Data and model statistics

Construct	WT (Yu)	WT	F101Y	F146Y	F42W	F101W	F146W	WWW
<i>Data statistics</i>								
Unit cell dimensions (Å)								
<i>a</i> = <i>b</i>	55.0	55.0	55.0	54.9	54.9	55.1	54.9	55.0
<i>c</i>	77.2	76.8	77.1	77.3	77.2	76.7	77.2	76.7
Space group	<i>P</i> 43							
Resolution range (Å)	55.0–2.28	55.0–2.1	44.8–2.1	54.9–2.26	54.9–2.34	55.1–2.1	54.9–2.1	55.0–2.34
Observed reflections	10,313	13,359	13,433	10,788	9723	13,419	13,286	9703
Completeness (%)	100	100	100	100	100	100	99	98
<i>I</i> / σ	?	24.0	37.0	22.3	29.6	23.6	14.1	17.9
<i>R</i> _{sym}	0.056	0.054	0.054	0.068	0.071	0.065	0.09	0.073
<i>Atomic model statistics</i>								
<i>R</i> _{crys} (%)	15.7	18.3	18.3	18.0	19.3	18.2	18.5	
<i>R</i> _{free} (%)	21.3	20.8	19.9	19.2	22.5	20.9	19.9	22.9
Bond length RMS (Å)	0.013	0.006	0.005	0.006	0.006	0.005	0.005	0.006
Bond angle RMS (deg.)	2.13	1.45	1.45	1.40	1.35	1.34	1.33	1.30
RMSD (Yu)	–	0.20	0.22	0.22	0.37	0.33	0.36	0.45
Cavity volume (Å ³)	88.0	84.2	84.9	96.6	108.5	95.67	82.93	108.9

WT (Yu) values were taken from Yu *et al.*, 1999.² WT represents our wild-type data and refined model. IL-1 β wild-type statistics were again obtained from Yu *et al.*²

F101Y

The phenolic hydroxyl group finds a hydrogen-bonding partner with the sulfhydryl group of cysteine 71. The distance between these moieties is 3.23 Å. The CB–SG–OH angle is 124° while the CZ–OH–SG angle is 95°. It also resides near the backbone carbonyl group of leucine 69 (3.4 Å) but the geometry (OH–O–C=78°) is not conducive to hydrogen bond formation (Figure 5).

F146Y

The hydroxyl group is hydrogen bonded to the backbone carbonyl group of leucine 122 2.7 Å away. The O–OH–CZ angle is 116° and the OH–O–C angle is 105° (Figure 6).

F42W

The indole nitrogen atom introduced by this

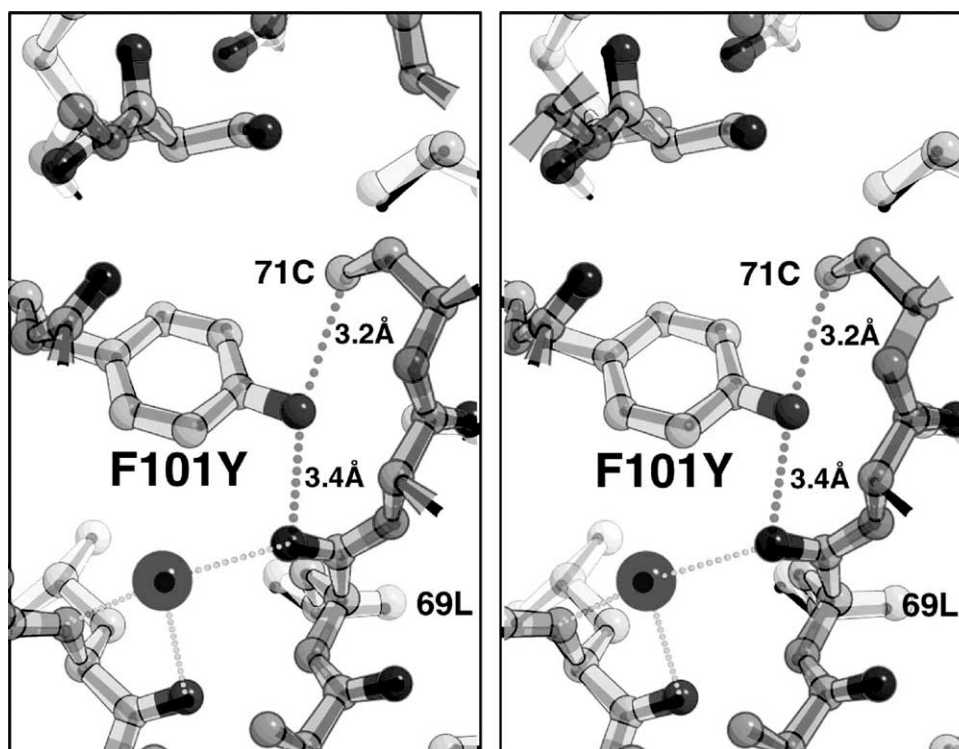


Figure 5. Local structure of F101Y around the mutation site. The stereograph ball and stick model of the mutant structure is shown superposed over the darker, smaller, wild-type structure. Large dark spheres represent water molecules. Dotted lines represent putative hydrogen bonds.

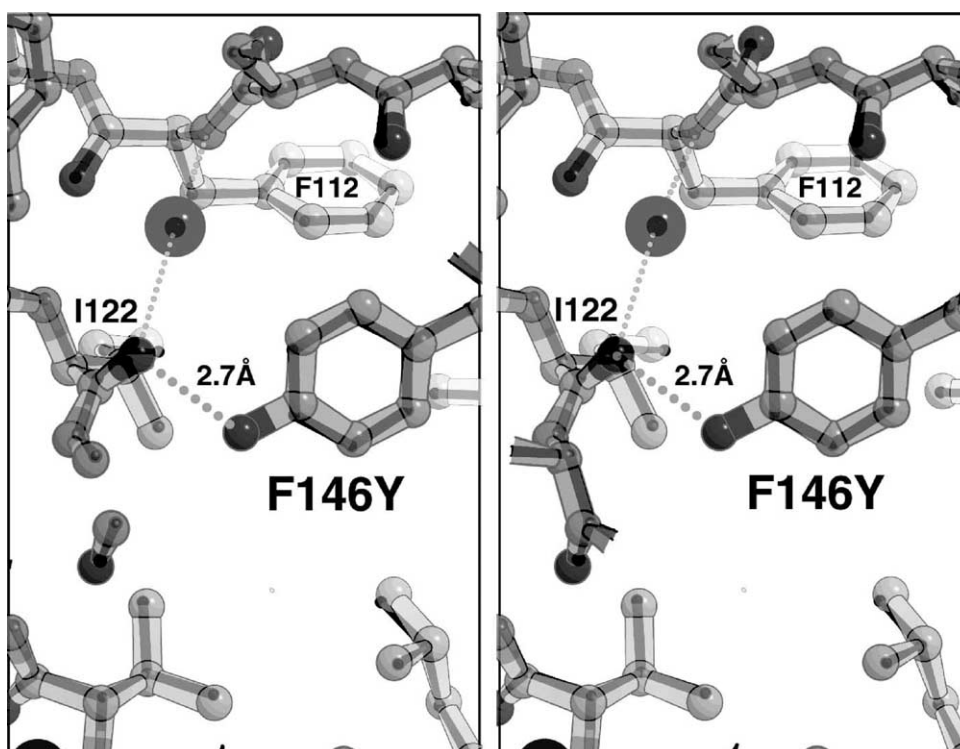


Figure 6. Local structure of F146Y around the mutation site. The stereograph ball and stick model of the mutant structure is shown superposed over the darker, smaller, wild-type structure. Large dark spheres represent water molecules. Dotted lines represent putative hydrogen bonds.

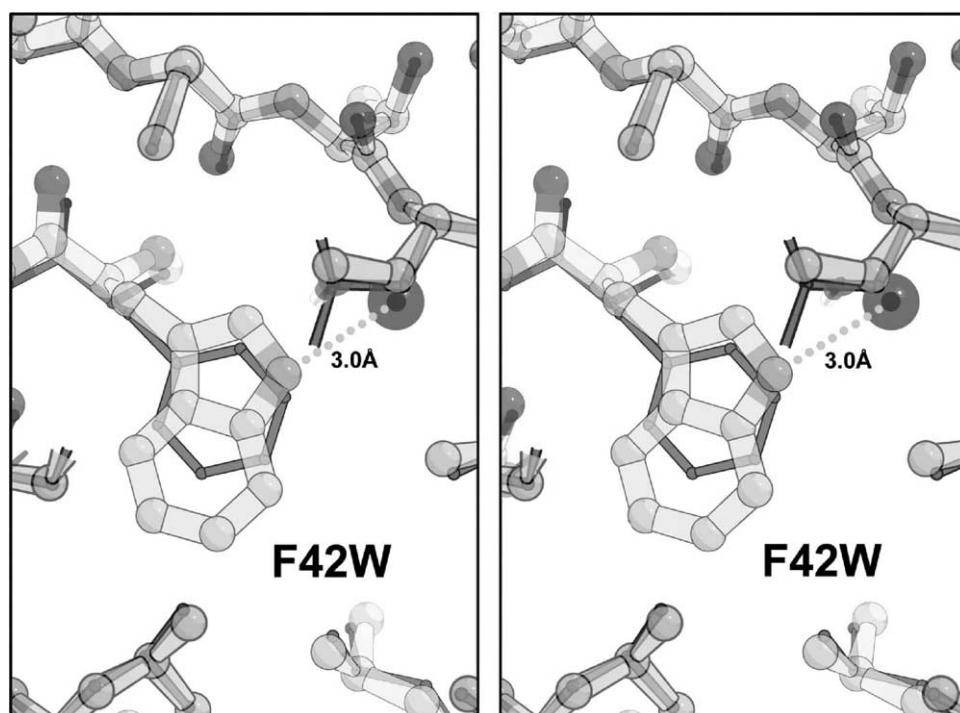


Figure 7. Local structure of F42W around the mutation site. The stereograph ball and stick model of the mutant structure is shown superposed over the darker, smaller, wild-type structure. Large dark spheres represent water molecules. Dotted lines represent putative hydrogen bonds.

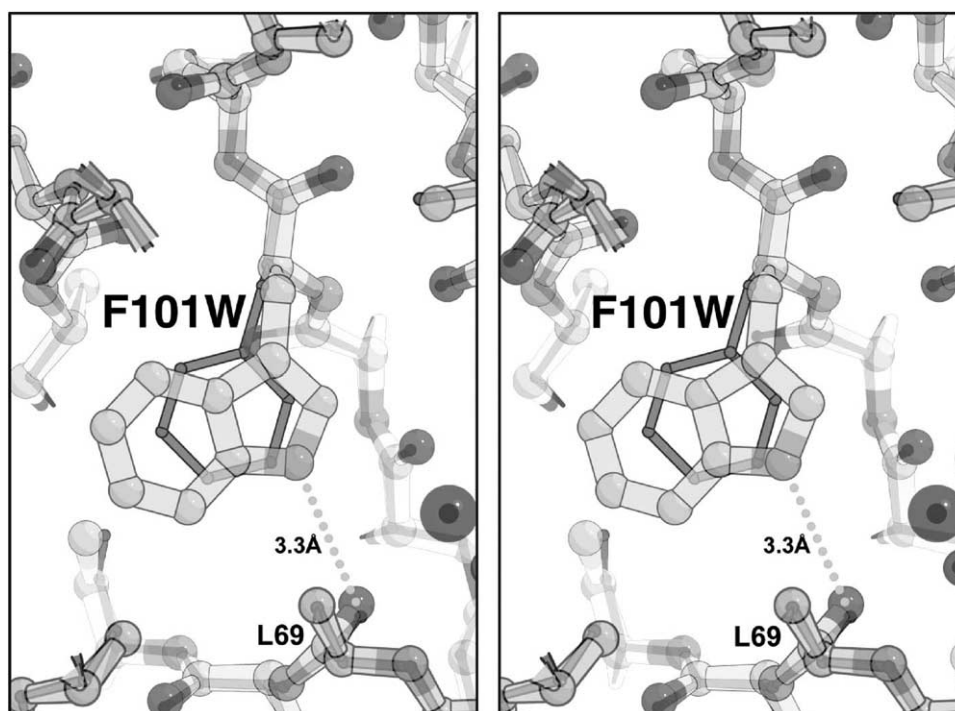


Figure 8. Local structure of F101W around the mutation site. The stereographic ball and stick model of the mutant structure is shown superposed over the darker, smaller, wild-type structure. Large dark spheres represent water molecules. Dotted lines represent putative hydrogen bonds.

mutation finds a hydrogen-bonding partner in an existing water molecule 3.0 Å away, outside of the cavity but buried in the protein core (Figure 7).

F101W

The introduced indole nitrogen atom in this mutation finds a hydrogen bond acceptor from the

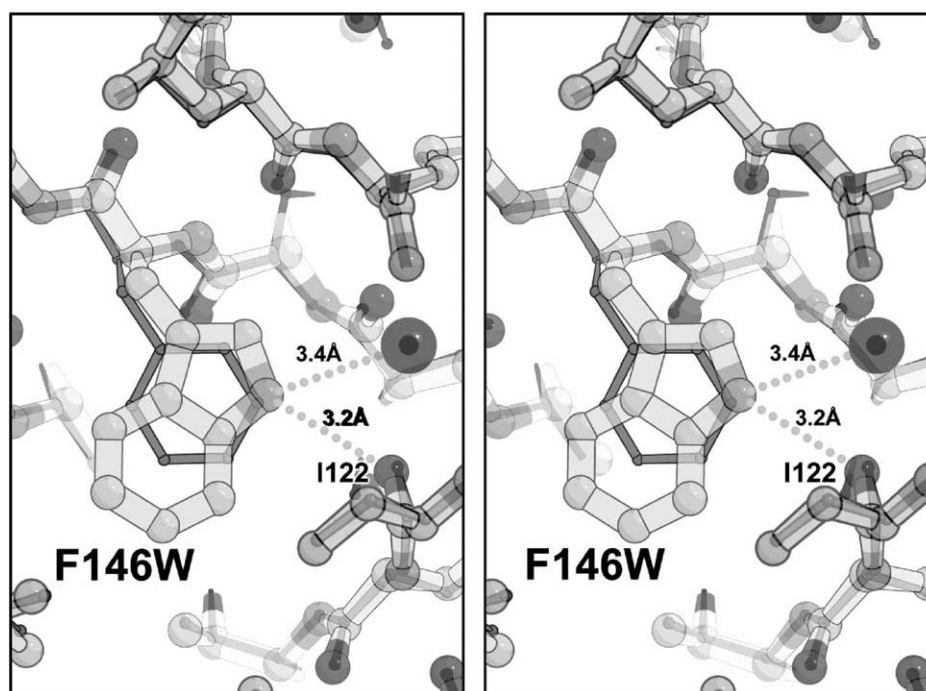


Figure 9. Local structure of F146W around the mutation site. The stereographic ball and stick model of the mutant structure is shown superposed over the darker, smaller, wild-type structure. Large dark spheres represent water molecules. Dotted lines represent putative hydrogen bonds.

Table 3. Free energy differences of transfer to organic solvent

Residue (reference: Phe)	$\Delta\Delta G_{\text{H}_2\text{O}\rightarrow\text{C}_6\text{H}_{14}}$ (kJ/mol)	$\Delta\Delta G_{\text{H}_2\text{O}\rightarrow\text{C}_8\text{H}_{18}\text{O}}$ (kJ/mol)	$\Delta\Delta G_{\text{H}_2\text{O}\rightarrow\text{Vac}}$ (kJ/mol)
Tyr	-13.04	-4.77	-22.38
Trp	-2.72	2.59	-21.42
Leu	8.11	0.54	12.72
Ile	8.11	0.04	12.18

$\Delta\Delta G$ values are in reference to phenylalanine. Positive values indicate a more energetically favorable transfer. Values were obtained from Sharp *et al.*¹⁸

carbonyl group of leucine 69, 3.35 Å away. Another potential partner is a water molecule 3.5 Å away (Figure 8).

F146W

In this position the indole nitrogen atom also finds a similar pairing to that of the F101W mutation, in that it is bound to the carbonyl group of isoleucine 122 and is situated approximately 3.4 Å from a water molecule (Figure 9).

Discussion

The wall of the cavity in IL-1 β is formed by 15 carbon atoms from seven aliphatic residues and three phenylalanine residues. Two groups have reported the presence of positionally disordered water in this entirely hydrophobic cavity.^{2,4} In order to understand better the hydrophobic nature of the cavity we have examined the effects on the protein's structure and stability of mutation that modify the local hydrophobic character in the cavity. The three phenylalanine residues targeted in this study form a pseudo-triad about the cavity whose alpha carbon atoms are nearly equidistant (Figure 1). Each residue is exposed to the cavity to a different extent. All atoms of phenylalanine 101 are inaccessible from the cavity to a water-sized molecule. Only the Z carbon of phenylalanine 42 is exposed to the cavity, and nearly an entire face of the ring of phenylalanine 146 is exposed to the cavity.

Hydrophobicity of the cavity

The hydrophobic effect is considered the primary energetic force stabilizing the native structure of a protein.²⁴ Still, a quantitative description of the hydrophobic effect in regards to protein folding and stability remains out of reach. Hydrophobicity most often is discussed in terms of the energetics of transferring a fluid chemical compound from an organic non-polar solvent to water.^{25,26} It is an enticing idea that the hydrophobic effect in regards to protein stability can be quantified by examination of the component amino acids of a protein with regards to their associated energetic costs of transfer from some protein-like non-polar solvent to water. The most commonly referenced apolar compounds used to represent the environment

inside of a protein are cyclohexane and octanol (Table 3).^{3,18,19,27,28}

The tyrosine mutations had significant effects on the protein stability. Mutants F101Y and F146Y both showed approximately the same destabilizing effect as a result of the introduced phenolic hydroxyl group (7–10 kJ/mol). This is slightly less than would be expected assuming the protein were similar to a pure hydrocarbon environment, comparable to cyclohexane. Octanol is a commonly used reference solvent, as it is slightly more polar than cyclohexane and as such considered to better model the protein interior.^{5,8,29} However, the respective transfer energies between water and octanol considerably underestimate the observed destabilization. Examination of the crystal structures reveals that the phenolic hydroxyl groups in both proteins are situated near polar groups, which can serve as hydrogen bonding partners. In neither case does the phenolic hydroxyl group form a hydrogen bond to water in the cavity. F42Y was considerably less stable than its sister mutants, with an estimated $\Delta\Delta G$ of between -16 and -20 kJ/mol. Examining the mutation by computer modeling offers some explanation for the difference in stability relative to the other two mutant constructs. The hydroxyl moiety in this case would be wedged between the C ^{δ 1} atoms of leucine residues 18 and 26, projecting into the cavity. In contrast to the other two-tyrosine models there would be no access to any polar protein atoms for this hydroxyl group. However, in the model it is situated such that it could interact with water in the cavity. The severe cost to the stability of the protein suggests that this does not occur. In fact the estimated energetic cost indicates that the environment maintains a dielectric of something between that of cyclohexane and a gas. This would correspond to a free energy cost of between -13.8 and -22.4 kJ/mol.

The tryptophan mutants were much better behaved, though they too were less stable than the wild-type protein. The $\Delta\Delta G$ values for F42W and F101W, -3.0 and -2.6 kJ, respectively, corresponding quite well to what would be expected from a hydrocarbon environment. F146W, however, proved nearly as stable as the wild-type protein. All maintain hydrogen bonds to the indole nitrogen atoms. The surprising observation, however, is that of the one maintaining the closest, and presumably the most energetically favorable hydrogen bond from that nitrogen is the least stable. This indicates

that difference in stability does not completely reflect the apolar nature of the environment.

The aliphatic replacement mutants were constructed after considering the adverse response of the protein to the more polar replacement mutants. Based on the apparent hydrophobic environment it was assumed that the protein would be amenable to a more hydrophobic replacement. Remarkably, these were devastating to the protein. Clearly factors other than hydrophobicity must be considered, when describing the environment in and about the cavity of IL-1 β .

Packing and cavities

Cyrus Chothia observed that there is a correlation between the solvent-accessible surface areas of the amino acid side-chains and the hydrophobicity as defined in terms of the free energy change from organic solvent to water.³⁰ He found that the hydrophobicity of residues in proteins is approximately 100 J/mol per \AA^2 of accessible surface area. In other words the energetic cost is proportional to the surface area of the cavity created in water. This applies as well to polar side-chains as long as those groups are hydrogen bonded.³¹ Eriksson *et al.* approached the problem by studying the structural and energetic effects of making artificial cavities in the protein, bacteriophage T4 lysozyme. This was accomplished by replacing leucine with alanine at a number of sites in the core of the protein.⁸ The energetic costs of the various mutants were found to be linearly correlated to the solvent-accessible surface of the cavity created (~ 100 J/mol per \AA^2) with an added constant corresponding to the free energy difference associated with transferring the respective amino acids from octanol to water (~ 7.9 kJ/mol). In terms of the volume of the cavity created the cost was estimated to be about 84 J/mol per \AA^3 . This latter value has since permeated the field of protein stability studies and is frequently used to infer the costs of natural cavities and implemented in calculations to assess the likelihood of hydration of cavities.^{3,32} The analyses by Rashin *et al.* indicate that the appropriate value for the cost of natural cavities found in proteins is about 250 kJ/mol per \AA^3 .³³

The tryptophan mutants examined here were created in order to decrease the size of the cavity and in doing so confer some proportional amount of stability to the protein. None of the mutants revealed a significant decrease in the cavity size. In fact, in the case of F42W the cavity is significantly larger. All of the mutants appear to have hydrogen-bonding partners. The difference in cavity volume between F146W, (82.9 \AA^3) and F42W (108.5 \AA^3) is 25.6 \AA^3 . Using the estimate from Eriksson of 84 J/mol \AA^3 the free energy difference between these mutants would be expected to be about 2.2 kJ/mol. The calculated free energy difference determined calorimetrically is also 2.2 kJ/mol. Comparison of to F101W does not yield as

convincing results, as it is off by about 0.7 kJ/mol in comparison to the other two. This may reflect the difference in the relative hydrogen bond strengths. The hydrogen bond from the indole nitrogen atom of F101W is slightly longer and at a slightly less favorable angle compared to the respective interactions in the other two related mutants. However the magnitude of these details lies within the error of the models.

The crystallographically determined atomic models reveal that the indole rings all lie in the same plane as the benzyl groups they replace. The extra bulk is accommodated by the protein. Clearly the cavity comes with some energetic cost. So what energetic force makes the protein opt to absorb the extra bulk rather than placing it in the cavity? The residues defining the cavity wall in all of the refined models have some of the lowest thermal factors in the protein and reveal some of the lowest RMS displacements with respect to the wild-type protein. This is consistent with the observation that atoms defining cavities in proteins, in general, tend to be very inflexible.¹¹ This suggests that these residues are less fluid and may not compensate for large packing rearrangements as well as the interior regions of the protein. This still does not account for the magnitude of destabilization observed in the aliphatic replacement mutants. The difference in volume between phenylalanine and leucine or isoleucine is approximately 27 \AA^3 .^{3,34} The resulting free energy differences assuming a cavity formation of this size and based on the relevant values from Eriksson & Rashin are ~ 2.3 kJ/mol and ~ 6.7 kJ/mol, respectively. The energetic costs of all of the aliphatic mutants examined here clearly exceed these values. Furthermore, as mentioned above, the relative hydrophobicities of leucine and isoleucine compared to that of phenylalanine should be expected to stabilize the protein. Unfortunately, the limited stability of these mutants makes them difficult to quantitatively characterize.

Water in the cavity

No ordered water molecules were observed within the cavities of any of the high-resolution structures examined in this report. This is consistent with all of the IL-1 β models deposited in the PDB. However, two reports indicate the presence of positionally disordered water that eluded standard crystallographic identification due to their diffuse nature. There are some notable features to the IL-1 β cavity and the solvent therein that deserve to be looked at. The cavity is large enough to accommodate about four water molecules without bad contacts.² Even under optimal geometric constraints, in a cavity this size, four water molecules would suffer a dramatic loss in entropy relative to bulk water, due to immobilization. On the other hand it is not likely that a single water molecule would be energetically favorable in such a low dielectric environment. A water dimer would be

considerably more favored over a single water molecule.³⁵ This is consistent with previous findings that indicate the presence of approximately two water molecules in the cavity.

It has been suggested that the phenylalanine residues in the cavity may contribute to the stabilization of the water. There are three phenylalanine residues in the cavity. Aromatic moieties are often found forming hydrogen bonds in protein structures and have been shown to hydrogen bond to water.³⁶ Hydrogen bonds to aromatic groups are typically longer (3.4–3.7 Å) and less rigid than other hydrogen bonds. Furthermore, they are less directional dependent as they can be formed to any of the atoms of the aromatic group. The center of mass of the density in the cavity of IL-1 β , as determined by Yu *et al.*, is between 4.5 and 5.0 Å from the exposed atoms of the phenylalanine residues in the cavity. That is longer than what would be expected for single water molecule at that position to make a hydrogen bond. If we consider that a dimer of water would have a radius approximately 1 Å greater than a single water molecule³⁷ then a reasonable hydrogen bonding distance could be achieved from that position to any of the aromatic atoms. The positioning of the phenylalanine residues around the cavity may allow for flexible hydrogen bonding system that can satisfy the electrostatic requirements of the water in the cavity and still allow for flexibility and mobility of the water thereby reducing the entropic cost that would otherwise result from more rigid, directional hydrogen bonding. In the beta-trefoil family of proteins the central cavity is a common feature. Furthermore, in the comparable positions to those examined here, aromatic groups are remarkably well conserved in these proteins. In most cases these positions are held by phenylalanine, but in some tryptophan residues are observed. Attempts to replace the phenylalanine residues with non-aromatic residues result in severe destabilization of the IL-1 β . These observations suggest that aromatic residues at those positions have some characteristic that is essential to the folding and stability of beta-trefoil type structures. That characteristic may be the flexible hydrogen bonding potential that they offer, as protein folding involves a complex and delicate balance between desolvation, hydration and the hydrophobic effect.

Materials and Methods

Mutagenesis and expression

Wild-type and mutant human IL-1 β were expressed in *Escherichia coli* strain BL-21 (DE3), carrying the expression plasmid pET 21a(+) containing the appropriate synthetic gene. Oligonucleotide primers, 33 bases long, containing a centrally located mutagenic codon were synthesized at the Biomolecular Analysis Synthesis and Sequencing laboratory at Florida State University.

The QuickChange (Stratagene) site-directed mutagenesis protocol was used to construct mutations

Phe42Tyr, Phe101Tyr, and Phe146Tyr. All DNA constructs were sequenced to confirm that the appropriate mutations and no misincorporations were made. *E. coli* cells transformed with the expression vectors were grown at 37 °C in LB medium to $A_{600\text{ nm}}=0.6$, at which time 1 mM isopropyl- β -D thiogalactopyranoside was added to the culture. After four more hours of growth the cells were harvested by centrifugation at 6000g for ten minutes. The cells were then resuspended in 100 mM Tris-HCl (pH 8.0), 5 mM benzamidine-HCl, 2.5 mM EDTA and lysed by French Press (1000 psi). The lysate was then centrifuged at 30,000g for 30 minutes. Wild-type IL-1 β was recovered from the lysis supernatant, while all mutant proteins were found in the pellets. All constructs were purified to high purity as indicated by a single band on a Coomassie brilliant blue-stained sodium dodecyl sulfate/polyacrylamide gel. Wild-type IL-1 β was purified following protocol previously published by Wingfield *et al.*³⁸ All of the mutant protein constructs were purified following resuspension of the lysis pellets in 100 mM Tris (pH 8.0), 2.5 mM EDTA, 14.3 mM 2-mercapto-ethanol (BME) and 5 M guanidinium chloride. The solution was then allowed to equilibrate overnight. The protein buffer was then exchanged by dialysis with 100 mM Tris (pH 7.4), 2.5 mM EDTA, 14.3 mM BME for refolding. The protein solution was then centrifuged 30,000g for 30 minutes. The supernatant was then applied to a column (98 cm \times 2.5 cm) of Ultragel AcA54 equilibrated with 100 mM Tris-HCl (pH 7.4). The column was eluted at 30 ml/hour and 12 ml fractions were collected. Crystals were grown from this solution. Samples for DSC were dialyzed against 50 mM sodium phosphate buffer (pH 6.5), 2 mM EDTA.

Differential scanning calorimetry

Calorimetric data were collected using a MicroCal model VP-DSC high-sensitivity differential scanning calorimeter. Sample conditions were optimized for equilibrium two-state thermal unfolding of the wild-type IL-1 β . The samples were examined in 50 mM sodium phosphate (pH 6.5), 2 mM Na₂EDTA, 0.7 M guanidinium chloride. All samples were filtered through a 0.22 μ m filter and degassed for ten minutes prior to loading into the instrument. The samples were kept under a constant pressure of 27 psi. All samples were examined at scan rate of 15 deg. C/hour. All buffer and protein scans were performed in triplicate and averaged. Data were collected using the MicroCal Origin DSC software package. Data were analyzed using a statistical mechanical two-state model with the software package DSCfit.³⁹ Native and denatured heat capacity curves were fit as first-order functions. The concentration constant *K* was constrained to a value of 1. All other parameters were iteratively fit to convergence.

Xray crystallography

Mutant constructs of IL-1 β were crystallized from 29% (w/v) ammonium sulfate and 100 mM Tris (pH 7.4) by hanging-drop, vapor-diffusion with protein concentrations between ~8 mg/ml and 10 mg/ml. Data were collected on an RAXIS-II imaging-plate detector using CuK α radiation at room temperature using 2° oscillations. The data were processed using the HKL software package. Model building and refinement were done using CCP4⁴⁰ and CNS⁴¹ using the coordinates from Bin *et al.*,² Protein Data Bank file 9ILB as the starting model.

Visualization for model analysis was done using O.⁴² Cavity calculations were done with CASTP.⁴³

Acknowledgements

We thank Eric Fontano for his assistance in constructing the computer graphics, and Balaji Bhyravbhatla, Thayumanasamy Somasundaram "Soma" and Alexei Soares for their helpful advice. This work was supported by U.S. Public Health Service Outstanding Investigator Grant CA47439 to D.L.D.C. from the National Cancer Institute and by a National Science Foundation Research Training Grant, DBI 9602233 to Florida State University.

References

- Otting, G., Liepinsh, E., Halle, B. & Frey, U. (1997). NMR identification of hydrophobic cavities with low water occupancies in protein structures using small gas molecules. *Nature Struct. Biol.* **4**, 396–404.
- Yu, B., Blaber, M., Gronenborn, A. M., Clore, G. M. & Caspar, D. L. (1999). Disordered water within a hydrophobic protein cavity visualized by X-ray crystallography. *Proc. Natl Acad. Sci. USA*, **96**, 103–108.
- Wolfenden, R. & Radzicka, A. (1994). On the probability of finding a water molecule in a nonpolar cavity. *Science*, **265**, 936–937.
- Ernst, J. A., Clubb, R. T., Zhou, H. X., Gronenborn, A. M. & Clore, G. M. (1995). Demonstration of positionally disordered water within a protein hydrophobic cavity by NMR. *Science*, **267**, 1813–1817.
- Xu, J., Baase, W. A., Baldwin, E. & Matthews, B. W. (1998). The response of T4 lysozyme to large-to-small substitutions within the core and its relation to the hydrophobic effect. *Protein Sci.* **7**, 158–177.
- Buckle, A. M., Henrick, K. & Fersht, A. R. (1993). Crystal structural analysis of mutations in the hydrophobic cores of barnase. *J. Mol. Biol.* **234**, 847–860.
- Buckle, A. M., Cramer, P. & Fersht, A. R. (1996). Structural and energetic responses to cavity-creating mutations in hydrophobic cores: observation of a buried water molecule and the hydrophilic nature of such hydrophobic cavities. *Biochemistry*, **35**, 4298–4305.
- Eriksson, A. E., Baase, W. A., Zhang, X. J., Heinz, D. W., Blaber, M., Baldwin, E. P. & Matthews, B. W. (1992). Response of a protein structure to cavity-creating mutations and its relation to the hydrophobic effect. *Science*, **255**, 178–183.
- Jackson, S. E., Moracci, M., elMasry, N., Johnson, C. M. & Fersht, A. R. (1993). Effect of cavity-creating mutations in the hydrophobic core of chymotrypsin inhibitor 2. *Biochemistry*, **32**, 11259–11269.
- Lee, J., Lee, K. & Shin, S. (2000). Theoretical studies of the response of a protein structure to cavity-creating mutations. *Biophys. J.* **78**, 1665–1671.
- Hubbard, S. J. & Argos, P. (1994). Cavities and packing at protein interfaces. *Protein Sci.* **3**, 2194–2206.
- Covalt, J. C., Jr, Roy, M. & Jennings, P. A. (2001). Core and surface mutations affect folding kinetics, stability and cooperativity in IL-1 beta: does alteration in buried water play a role? *J. Mol. Biol.* **307**, 657–669.
- Blaber, M., Lindstrom, J. D., Gassner, N., Xu, J., Heinz, D. W. & Matthews, B. W. (1993). Energetic cost and structural consequences of burying a hydroxyl group within the core of a protein determined from Ala→Ser and Val→Thr substitutions in T4 lysozyme. *Biochemistry*, **32**, 11363–11373.
- Dao-pin, S., Anderson, D. E., Baase, W. A., Dahlquist, F. W. & Matthews, B. W. (1991). Structural and thermodynamic consequences of burying a charged residue within the hydrophobic core of T4 lysozyme. *Biochemistry*, **30**, 11521–11529.
- Dwyer, J. J., Gittis, A. G., Karp, D. A., Lattman, E. E., Spencer, D. S., Stites, W. E. & Garcia-Moreno, E. B. (2000). High apparent dielectric constants in the interior of a protein reflect water penetration. *Biophys. J.* **79**, 1610–1620.
- Liggins, J. R., Lo, T. P., Brayer, G. D. & Nall, B. T. (1999). Thermal stability of hydrophobic heme pocket variants of oxidized cytochrome c. *Protein Sci.* **8**, 2645–2654.
- Maurus, R., Overall, C. M., Bogumil, R., Luo, Y., Mauk, A. G., Smith, M. & Brayer, G. D. (1997). A myoglobin variant with a polar substitution in a conserved hydrophobic cluster in the heme binding pocket. *Biochim. Biophys. Acta*, **1341**, 1–13.
- Sharp, K. A., Nicholls, A., Friedman, R. & Honig, B. (1991). Extracting hydrophobic free energies from experimental data: relationship to protein folding and theoretical models [published erratum appears in *Biochemistry* 1993. **32**, 5490. *Biochemistry*, **30**, 9686–9697].
- Zhang, C., Vasmatzis, G., Cornette, J. L. & DeLisi, C. (1997). Determination of atomic desolvation energies from the structures of crystallized proteins. *J. Mol. Biol.* **267**, 707–726.
- Makhatadze, G. I., Clore, G. M., Gronenborn, A. M. & Privalov, P. L. (1994). Thermodynamics of unfolding of the all beta-sheet protein interleukin-1 beta. *Biochemistry*, **33**, 9327–9332.
- Adamek, D., Popovic, A., Blaber, S. & Blaber, M. (1998). Denaturation studies of human acidic fibroblast growth factor. In *BioCalorimetry: Applications of Calorimetry in the Biological Sciences* (Ladbury, J. E. & Haq, I., eds), pp. 235–242. Wiley, New York.
- Blaber, S. I., Culajay, J. F., Khurana, A. & Blaber, M. (1999). Reversible thermal denaturation of human FGF-1 induced by low concentrations of guanidine hydrochloride. *Biophys. J.* **77**, 470–477.
- Heidary, D. K. & Jennings, P. A. (2002). Three topologically equivalent core residues affect the transition state ensemble in a protein folding reaction. *J. Mol. Biol.* **316**, 789–798.
- Dill, K. A. (1990). Dominant forces in protein folding. *Biochemistry*, **29**, 7133–7155.
- Tanford, C. (1980) *The Hydrophobic Effect*, 2nd edit, Wiley, New York.
- Murphy, K. P. & Gill, S. J. (1991). Solid model compounds and the thermodynamics of protein unfolding. *J. Mol. Biol.* **222**, 699–709.
- Radzicka, A., Pedersen, L. & Wolfenden, R. (1988). Influences of solvent water on protein folding: free energies of solvation of *cis* and *trans* peptides are nearly identical. *Biochemistry*, **27**, 4538–4541.
- Shortle, D., Stites, W. E. & Meecker, A. K. (1990). Contributions of the large hydrophobic amino acids to the stability of *staphylococcal nuclease*. *Biochemistry*, **29**, 8033–8041.
- Matthews, B. W. (1995). Studies on protein stability with T4 lysozyme. *Advan. Protein Chem.* **46**, 249–278.

30. Chothia, C. (1974). Hydrophobic bonding and accessible surface area in proteins. *Nature*, **248**, 338–339.
31. Richards, F. M. (1977). Areas, volumes, packing and protein structure. *Annu. Rev. Biophys. Bioeng.* **6**, 151–176.
32. Hubbard, S. J., Gross, K. H. & Argos, P. (1994). Intramolecular cavities in globular proteins. *Protein Eng.* **7**, 613–626.
33. Rashin, A. A., Iofin, M. & Honig, B. (1986). Internal cavities and buried waters in globular proteins. *Biochemistry*, **25**, 3619–3625.
34. Gerstein, M. & Richards, F. M. (1999). Molecular geometry and features. In *International Tables of Crystallography* (Rossmann, M. G., ed.), vol. F, Commission on International Tables, Aachen, Germany.
35. Xu, J., Baase, W. A., Quillin, M. L., Baldwin, E. P. & Matthews, B. W. (2001). Structural and thermodynamic analysis of the binding of solvent at internal sites in T4 lysozyme. *Protein Sci.* **10**, 1067–1078.
36. Steiner, T., Schreurs, A. M., Kanters, J. A. & Kroon, J. (1998). Water molecules hydrogen bonding to aromatic acceptors of amino acids: the structure of Tyr-Tyr-Phe dihydrate and a crystallographic database study on peptides. *Acta Crystallog. sect. D*, **54**, 25–31.
37. Jeffrey, G. A. & Sanger, W. (1994). *Hydrogen Bonding in Biological Molecules*, Springer, New York.
38. Wingfield, P., Payton, M., Tavernier, J., Barnes, M., Shaw, A., Rose, K. *et al.* (1986). Purification and characterization of human interleukin-1 beta expressed in recombinant *Escherichia coli*. *Eur. J. Biochem.* **160**, 491–497.
39. Grek, S., Davis, J. & Blaber, M. (2001). An efficient flexible-model program for the analysis of differential scanning calorimetry data. *Protein Pept. Letters*, **8**, 429–436.
40. Otinowski, Z. (1993). Oscillation data reduction program. In *Data Collection and Processing. CCP4 Daresbury Study Weekend* (Sawyer, L., Isaacs, N. & Bailey, S., eds), pp. 56–62, Daresbury Laboratory, Warrington, UK.
41. Brunger, A. T., Adams, P. D., Clore, G. M., DeLano, W. L., Gros, P., Grosse-Kunstleve, R. W. *et al.* (1998). Crystallography and NMR system: a new software suite for macromolecular structure determination. *Acta Crystallog. sect. D*, **54**, 905–921.
42. Jones, T. A., Zou, J. Y., Cowan, S. W. & Kjeldgaard, M. (1991). Improved methods for building protein models in electron density maps and the location of errors in these models. *Acta Crystallog. sect. A*, **47**, 110–119.
43. Liang, J., Edelsbrunner, H. & Woodward, C. (1998). Anatomy of protein pockets and cavities: measurement of binding site geometry and implications for ligand design. *Protein Sci.* **7**, 1884–1897.

Edited by P. Wright

(Received 8 July 2004; received in revised form 17 November 2004; accepted 18 November 2004)